14

Features of the development of a main crack in a natural heterogeneous material under mechanical loading, revealed using X-ray computed microtomography

© E.E. Damaskinskaya[1], V.L. Hilarov[1], Yu.S. Krivonosov[2], A.V. Buzmakov[2], V.E. Asadchikov[2], D.I. Frolov[1]

[1] Ioffe Institute,
St. Petersburg, Russia
[2] National Research Center „Kurchatov Institute“,
Moscow, Russia

E-mail: Kat.Dama@mail.ioffe.ru

Received October 23, 2025
Revised October 23, 2025
Accepted October 26, 2025

The aim of this study was to directly observe and analyze the morphological features of a main crack developing in samples of natural heterogeneous materials under mechanical stress. X-ray computed microtomography was used to detect defects in the volume. A unique feature of the experiments was that tomographic imaging was performed while the sample was under load. Based on the analysis of tomographic slices, three-dimensional models of the defect structure were constructed, the fractal dimension and relative volume of the microcrack system were calculated.

Keywords: X-ray computed microtomography, main crack evolution, fractal dimension, relative defect volume.

DOI: 10.61011/PSS.2026.02.63390.293-25

1. Introduction

Numerous experiments involving the deformation of brittle structurally heterogeneous materials of both natural and artificial origin indicate [1–8] that the fracture process in them occurs in a number of sequential stages. The main crack evolves at the final stage of this process.

This paper describes the study of the main crack propagation in specimens of natural heterogeneous materials under the action of a uniaxial compressive load. X-ray computer microtomography was used in the studies. This method allows to observe the defects arising in the volume of an opaque material, and, importantly, to further analyze the parameters of these defects.

Recently, computer tomography has become widespread in the study of microcracks formed as a result of mechanical action. As a rule, tomographic imaging is made either after mechanical tests or after each stage of loading [9–12]. The tomographic imaging in these experiments was held for the unloaded specimens. In [13,14] experiments are described, when tomographic studies of specimens in loaded state were performed. The cracks system development was observed with load increasing. However, no quantitative crack parameters were determined.

The objective of this study is to conduct direct observation and analysis of the morphological features of the main crack, which is initiated in the specimens of natural heterogeneous materials. A distinctive feature of the study is that the specimen is loaded throughout the experiment.

2. Experiment

Westerly granite, which is often used in rock deformation experiments, was chosen as the tested material [1,15,16]. However, direct observations and visualization of the development of the main fracture, as well as the determination of its morphological parameters, have not been performed before. Mineral components contained in Westerly are listed in the table below.

Specimen end faces were additionally polished to ensure their flatness. Lateral surface of specimens before experiments was fixed using heat shrink material to prevent spillage during deformation. The specimens were made as cylinders 7 mm in diameter and 14 mm high.

In order to trace the spread of the main crack (crack system), it is necessary to perform a tomographic imaging of the loaded specimen. A special portable loading device was designed (see Figure 1), which provides the necessary load, can be placed into the tomograph chamber and does not interfere with measurements (described in detail in [17]).

The load was applied to the specimen by rotating the screw. With the help of an electronic torque wrench, the torque is measured (which is later converted into the load).

Tomographic imaging was carried out using a cone-beam X-ray microtomograph „MICROTOM“, developed and designed at the Scientific Research Center „Kurchatov Institute“ [18]. In tomograph a microfocus polychromatic X-ray source with molybdenum shooting anode and focal spot size $15-20\,\mu$m was used. For the experiment accelerating voltage 80 kV was selected. Tomographic projections of

Mineral components of Westerly granite

Mineral	Quartz (Quartz)	Plagioclase (Plagioglase)	Fieldspar (K-Feldspar)	Biotite (Biotite)	Muscovite (Muscovite)
	28 %	33 %	33 %	3.5 %	1.9 %
Density, kg/m^3	2600–2650	2620–2760	2560	2800–3400	2760–3100

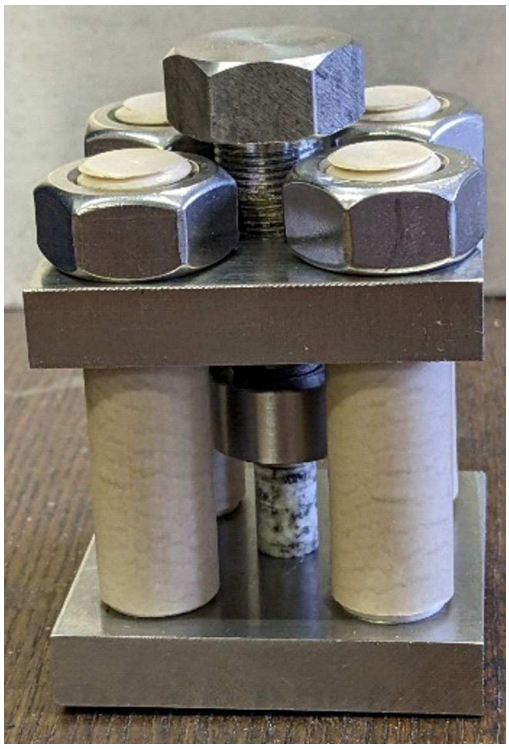

Figure 1. Photo of a portable load device with an installed specimen.

the specimen were recorded by XIMEA X-ray detector with a matrix of 2968×5056 elements and a pixel size of $8.5\,\mu$m. A series of tomographic experiments at all stages of the specimen destruction was performed in a single geometry: source-specimen distance — 50 mm and source–detector distance 200 mm, geometric magnification $M = 4.0$. In each experiment 720 projections were registered in range of angles 360°. 3D images of objects were restored using FDK algorithm [19]. To reduce the „cup effect", which is artifact and occurs due to the „hardening" of the polychromatic beam when passing through the specimen, Cu-filter 0.05 mm thick was installed between the source and the specimen. Besides, for complete removal of the cup-like artifact the procedure of automatic gamma — correction, described in paper [20], was applied to initially normalized and logarithmic sinograms. Also note that considering the suggested geometry of the experiment the specimen tomography was made not for the entire specimen, but for its central portion with a height of 6 mm.

3. Results and discussion

During these experiments the contrast is associated with X-rays absorption during passage through the studied object. As the specimen material is heterogeneous, the absorption coefficients of different components differ. As a result, after tomographic reconstruction we obtain images of X-ray optical density distribution (see the shades of gray) in different horizontal sections of the specimen.

The experiment was performed in several stages. The load exerted on the specimen was gradually increased with a step of 0.5 kN. Tomographic imaging was performed after each change of the load. Examples of tomographic sections at the same specimen height are shown in Figure 2. No cracks were detected up to the load of $F = 9$ kN. When the load reached 9 kN, microcracks were detected in the specimen. Tomographic sections corresponding to this load are shown in Figure 2, *b*. Then the specimen was exposed to a load of 9 kN for a day. At the next stage, when turning the screw of the loading device, it was possible to achieve only a load of 8.1 kN, since under this load the specimen began to collapse intensively. We believe that formation of cracks led to stress relaxation in the material. That is why further development of the defect structure (the spread of cracks and the formation of new ones) occurred at lower loads. This hypothesis is fully confirmed by the data of tomographic studies of the specimen. Tomographic sections corresponding to this load of 8.1 kN are shown in Figure 2, *c*. It can be seen that the crack system has become more branched; in addition, cracks have appeared that were not observed at the previous stage of loading.

Next, using the same loading scheme other 3 loading stages were applied (7.1, 5.9 and 2.7 kN). Once again, we emphasize that in the experiment, at each subsequent stage of destruction, the load applied to the specimen was declining. Examples of tomographic sections obtained under these loads are shown in Figure 2, *d–f*. Thus, the evolution of the system of cracks that form the main crack is clearly traced.

To quantify the morphology of the crack system, the fractal dimension and the relative volume of the cracks were calculated.

Fractal dimension was found by method of box counting (BCM) [12,21,22]. The graph of the amount of cubes on the material-crack boundary versus the cube side length was plotted. This dependence was approximated by the power law dependence and the exponent gave the estimated fractal dimension. Substantially, this dimension D_0 is from the set

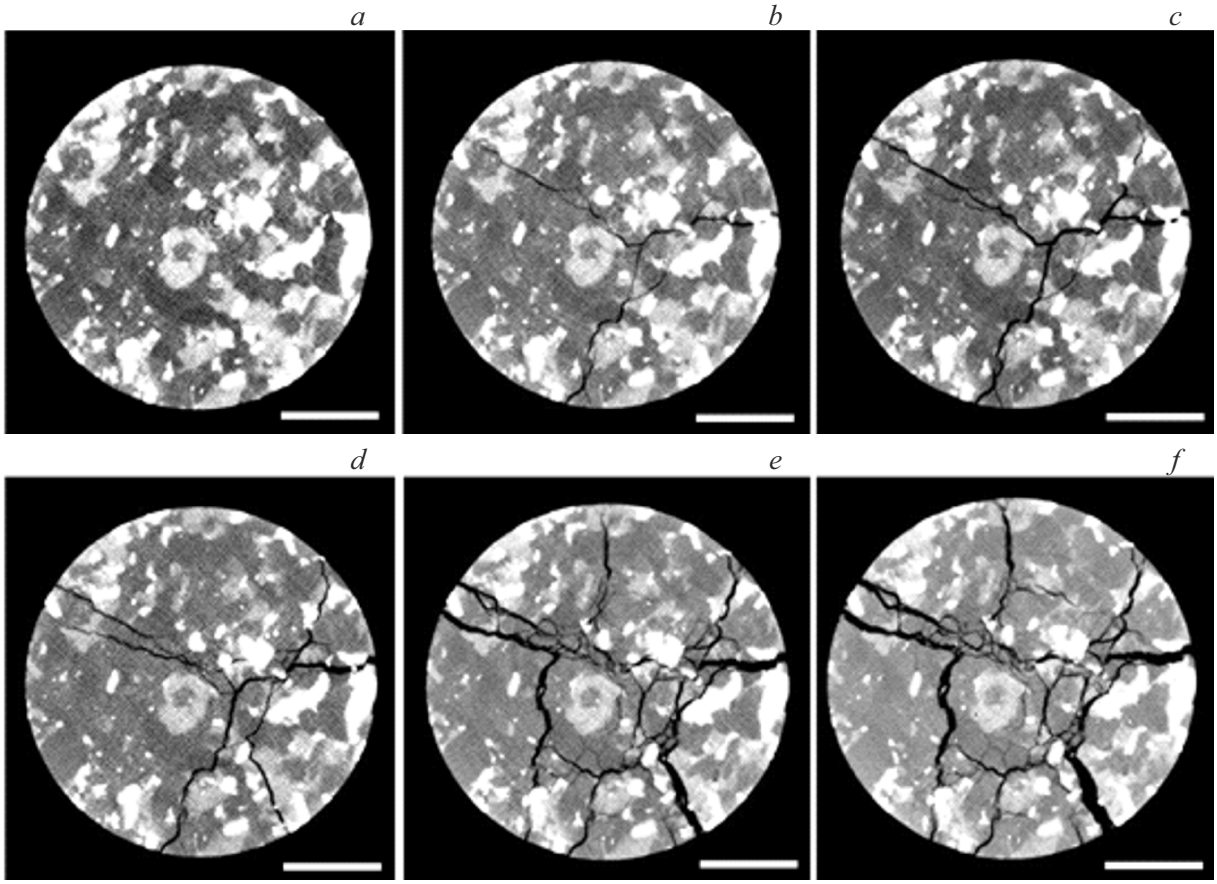

Figure 2. Tomographic sections of the specimen in shades of gray: *a*) initial specimen; *b, c, d, e, f*) specimen after each stage of loading. The length of the groove is 2 mm.

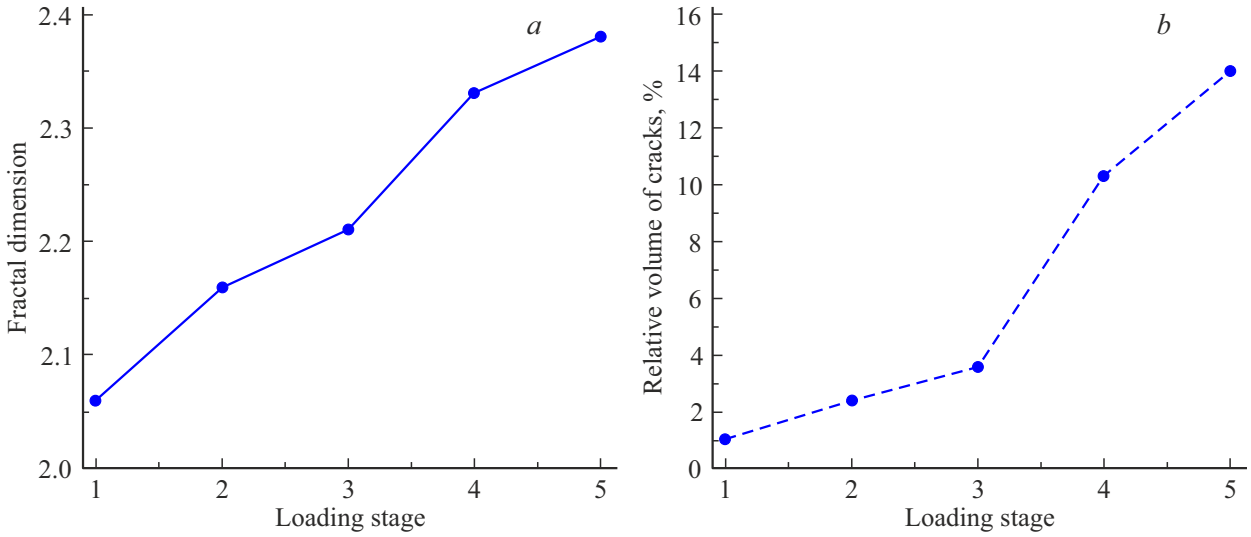

Figure 3. Values of *a*) fractal dimension and *b*) relative volume of cracks in the entire studied part of the specimen at each stage of loading.

of Renyi fractal dimensions [23]. Using this method we calculated the fractal dimension of the surfaces of cracks based of three-dimension models of cracks reconstruction. It can be seen that the fractal dimension of the crack system is gradually rising (Figure 3, *a*). At the first stage, the fractal dimension is 2.06, i. e. the crack is almost flat. At the final stage, the crack shape becomes more „bulky“, and the fractal dimension reaches 2.38.

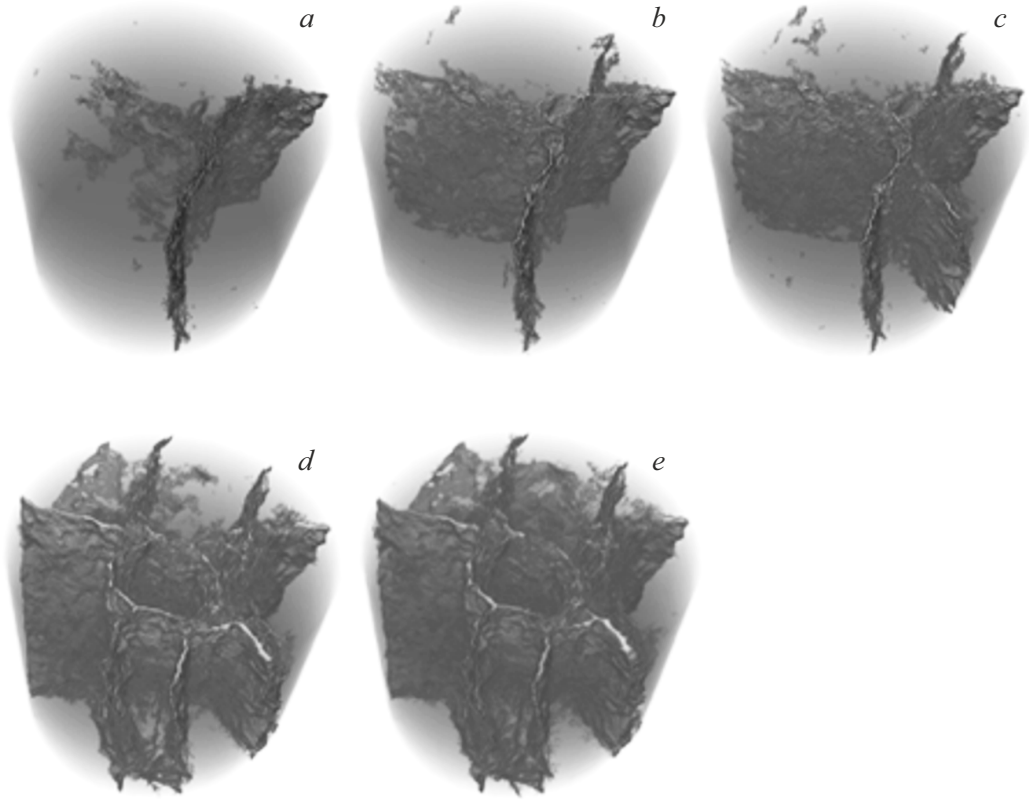

Figure 4. Three-dimensional visualization of the microcrack system at each of the 5 loading stages: *a*–*e* Dark gray objects of complex geometry inside the specimen — a formed crack.

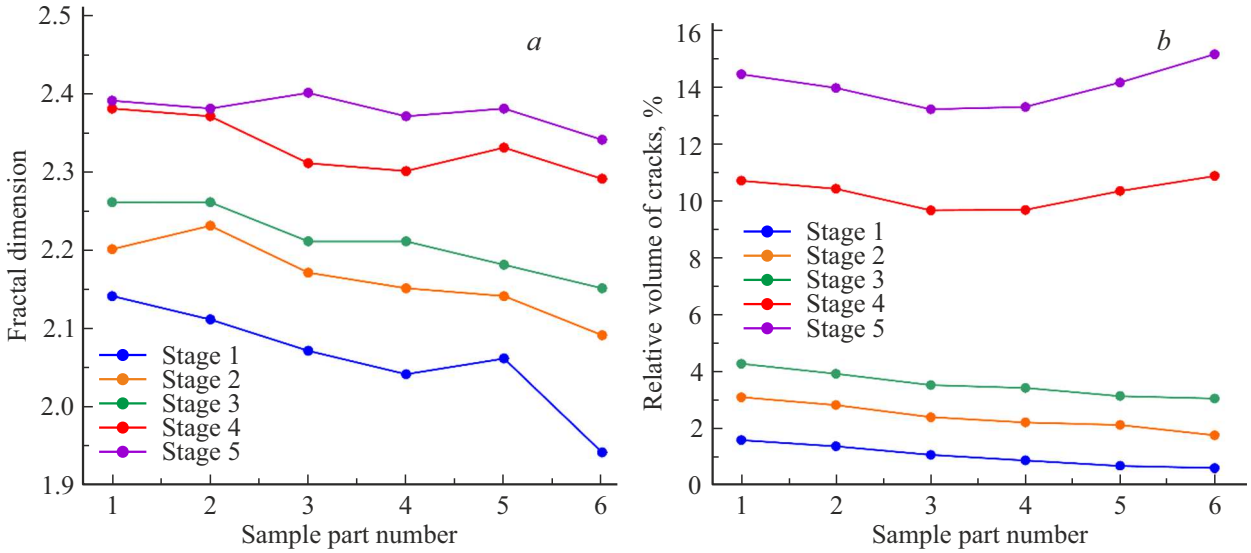

Figure 5. Values of *a*) fractal dimension and *b*) relative volume of cracks in the individual parts of the specimen at each stage of loading.

Relative volume is another quantitative parameter characterizing the crack. We may see that this parameter also rises from 1.1 % to 14.1 % (Figure 3, *b*).

An increase in the fractal dimension and relative volume of cracks indicates that the crack system is becoming more branched, occupying more volume. This is clearly illustrated by a tree-dimensional image of the microcracks system as seen from the tomography data (Figure 4).

Further, the changes in the fractal dimension and relative volume in different parts of the studied specimen's portion

at each stage of loading were analyzed in detail. To do this, the entire data set was divided into 6 parts according to the height of the specimen. The height of each part was 0.935 mm (147 tomography sections). Variation of these parameters is shown in Figure 5. It can be seen that in the first three stages, the fractal dimension varies in the height of the specimen (the crack forms differently in different regions). In the last stages, the fractal dimension has grown significantly and has become almost the same throughout the specimen. The relative volume of cracks at each stage demonstrates a low variability in the height of the specimen. There is a significant increase in relative volume in the last two stages.

Thus, the results obtained indicate that the crack system is gradually becoming more „bulky" (reaching the average value of the fractal dimension 2.38 according to the specimen), and the relative volume of cracks is rising.

4. Conclusion

A change in the morphology of the main crack in a specimen of Westerly granite under its mechanical loading has been investigated. Direct monitoring of defects in an opaque loaded specimen was provided by X-ray computer microtomography. Based on the analysis of tomographic sections, the fractal dimension and the relative volume fraction of the crack system at five loading stages were analyzed. Both parameters tend to grow amid the backdrop of the defective structure progress. This shows that the microcracks system becomes more developed and gradually occupies an ever larger volume. This conclusion is illustrated by the constructed three-dimensional models of the defect structure.

Funding

The objective of this work was set and the results were analyzed within the State assignment of Ioffe Physical-Technical Institute. The study was carried out within the State assignment of the SRC „Kurchatov Institute" regarding tomographic experiments and under the Agreement No. 075-15-2025-458 with the Ministry of Science and Higher Education of the Russian Federation regarding the mathematical processing of tomographic data.

Conflict of interest

The authors declare that they have no conflict of interest.

References

[1] D.A. Lockner, J.D. Byerlee, V. Kuksenko, A. Ponomarev, A. Sidorin. Nature **350**, *6313*, 39 (1991).
[2] L.R. Botvina. Fizika Zemli, **10**, 5 (2011) (in Russian).
[3] M. Petružálek, J. Vilhelm, V. Rudajev, T. Lokajíček, T. Svitek. Int. J. Rock Mech. Mining Sci. **60**, 208 (2013).
[4] Y. Hamiel, O. Katz, V. Lyakhovsky, Z. Reches, Yu. Fialko. Geophys. J. Int. **167**, 1005 (2006).
[5] V. Kuksenko, N. Tomilin, E. Damaskinskaya, D. Lockner. Pure Appl. Geophys. **146**, *2*, 253 (1996).
[6] V.B. Smirnov, A.V. Ponomarev, P. Bernar, A.V. Patonin. Fizika Zemli, **2**, 17 (2010) (in Russian).
[7] X. Lei, S. Ma. Earthq. Sci. **27**, *6*, 627 (2014).
[8] Y. Tal, T. Goebel, J.P. Avouac. Earth & Planetary Sci. Lett. **536**, 116133 (2020).
[9] S.-Q. Yang, P.G. Ranjith, Y.-L. Gui. Geotech. Test. J. **38**, *2*, 179 (2015).
[10] S. Zabler, A. Rack, I. Manke, K. Thermann, J. Tiedemann, N. Harthill, H. Riesemeier. J. Structural Geology. **30**, *7*, 876 (2008).
[11] Y. Zuo, Z. Hao, H. Liu, C. Pan, J. Lin, Z. Zhu, W. Sun, Z. Liu. Arab. J. Geosci. **15**, *22*, 1673 (2022).
[12] Y. Yang, Y. Ju, F. Li, F. Gao, H. Sun. J. Natural Gas Sci. Eng. **32**, 415 (2016).
[13] X.P. Zhou, Y.X. Zhang, Q.L. Ha. Theor. Appl. Fracture Mechanics **50**, *1*, 49 (2008).
[14] J.X. Ren. Soil and Rock Behavior and Modeling. https://doi.org/10.1061/40862(194)34
[15] J. Tullis, R.A. Yund. J. Geophys. Res. **82**, *36*, 5705 (1977).
[16] R.M. Stesky. Can. J. Earth. Sci. **15**, *3*, 361 (1978).
[17] E.E. Damaskinskaya, V.L. Gilyarov, Yu.S. Krivonosov, A.V. Buzmakov, V.E. Asadchikov, D.I. Frolov. FTT **66**, *9*. 1407 (2024).
[18] Yu.S. Krivonosov, A.V. Buzmakov, M.Yu. Grigoriev, A.A. Rusakov, Yu.M. Dymshits, V.E. Asadchikov. Kristallografiya **68** *1*, 160 (2023) (in Russian).
[19] L.A. Feldkamp, L.C. Davis, J.W. Kress. J. Opt. Soc. Am. A **1**, *6*, 612 (1984).
[20] A.S. Ingacheva, M.V. Chukalina. Math. Problems. Eng. ID 1405365 (2019).
[21] Y. Ju, J. Zheng, M. Epstein, L. Sudak, J. Wang, X. Zhao. Comput. Methods Appl. Mech. Eng. **279**, *7*, 212 (2014).
[22] H.P. Xie. Fractals in Rock Mechanics. CRC PRESS, Boca Raton (1993). 464 pp.
[23] R.D. Peng, Y.C. Yang, Y. Ju, L.T. Mao, Y.M. Yang. Chinese Sci Bull. **56**, *31*, 3346 (2011).

Translated by T.Zorina